



OPEN ACCESS

Localization of breakage points in knotted strings

To cite this article: Piotr Pieranski *et al* 2001 *New J. Phys.* **3** 10

View the [article online](#) for updates and enhancements.

You may also like

- [Review: knots and other new topological effects in liquid crystals and colloids](#)
Ivan I Smalyukh
- [Comparative analysis of the folding dynamics and kinetics of an engineered knotted protein and its variants derived from HP0242 of *Helicobacter pylori*](#)
Liang-Wei Wang, Yu-Nan Liu, Ping-Chiang Lyu et al.
- [Construction and application of knotted acoustic fields with intensity maxima](#)
Ya Liu, Weixuan Zhang and Xiangdong Zhang

Localization of breakage points in knotted strings

**Piotr Pieranski^{1,2}, Sandor Kasas³, Giovanni Dietler^{4†},
Jacques Dubochet⁵ and Andrzej Stasiak⁵**

¹ Department of Technical Physics, Poznan University of Technology,
60-965 Poznan, Poland

² Institute of Molecular Physics, 60-159 Poznan, Poland

³ Institute of Cell Biology and Morphology, University of Lausanne,
CH-1005 Lausanne, Switzerland

⁴ Institute of Condensed Matter Physics, University of Lausanne,
CH-1015 Lausanne, Switzerland

⁵ Laboratoire d'Analyse Ultrastructurale, University of Lausanne,
CH-1015 Lausanne, Switzerland

E-mail: giovanni.dietler@ipmc.unil.ch

New Journal of Physics **3** (2001) 10.1–10.13 (<http://www.njp.org/>)

Received 10 January 2001, in final form 17 April 2001

Published 14 June 2001

Abstract. It is a common macroscopic observation that knotted ropes or fishing lines under tension easily break at the knot. However, a more precise localization of the breakage point in knotted macroscopic strings is a difficult task. In the present work, the tightening of knots was numerically simulated, a comparison of strength of different knots was experimentally performed and a high velocity camera was used to precisely localize the site where knotted macroscopic strings break. In the case of knotted spaghetti, the breakage occurs at the position with high curvature at the entry to the knot. This localization results from joint contributions of loading, bending and friction forces into the complex process of knot breakage. The present simulations and experiments are in agreement with recent molecular dynamics simulations of a knotted polymer chain and with experiments performed on actin and DNA filaments. The strength of the knotted string is greatly reduced (down to 50%) by the presence of a knot, therefore reducing the resistance to tension of all materials containing chains of any sort. The present work with macroscopic strings reveals some important aspects, which are not accessible by experiments with microscopic chains.

† Author to whom correspondence should be addressed.

1. Introduction

Rock climbers and anglers know that a simple overhand knot tied on a mountaineering rope or a fishing line weakens it substantially [1, 2]. Ashley [1] reports that ‘a rope is weakest just outside the entrance of the knot’. However, this description of the localization of breakage points is hardly precise. Recently studies of knot breaking were extended to molecular dimensions. Arai *et al* [3] demonstrated that knotted actin filaments easily break within the knotted region. Saitta *et al* [4] performed molecular modelling studies demonstrating that knotted polyethylene chains break at the entrance of the knot, whereby they precisely mapped the strain energy distribution within a knot. Moreover, Taylor [5] recently discovered that certain proteins contain knots. The reasons to study this type of phenomena are that knots are present in synthetic as well as in biological polymers and can significantly weaken the resistance to traction of these materials. Concerning DNA, there is a battery of topoisomerases (enzymes) which are responsible for unknotting DNA, proving that living matter can deal with knots [6]. Although the breaking of knotted strings is well established, there have been no dedicated studies aimed to explain the reason of this breaking. In the present study experimental breaking of knotted fishing lines or knotted cooked spaghetti was compared with numerical simulation of tight knots in order to exactly determine the breakage point. We observe that the breakage point coincides with the point of high curvature of the string just inside the entrance to the knot. Thus, the main reason of the weakening of a knotted string is the curvature of the string. In the results section a justification of using cooked spaghetti for the experiments will be given, so that the present experiments are not so extravagant as might appear at first glance.

2. Materials and methods

2.1. Knot tightening simulations

Tightening of the open knots was performed with an appropriately modified SONO (shrink-on-no-overlaps) algorithm developed by one of the authors [7]. The algorithm simulates a process in which a rope with a knot slowly shrinks. The simulated rope is ideal, i.e. perfectly flexible but at the same time perfectly hard. Its perpendicular sections have the shape of discs of a fixed radius R . None of the sections are allowed to overlap. If this condition is fulfilled, the surface of the rope remains smooth and self-avoiding.

For obvious reasons the description of the simulated rope is discrete. The continuous axis K of the rope is approximated by a sequence of equidistant points $\{\mathbf{r}_i\}$, $i = 1, \dots, N$. In what follows we shall refer to the points as *nodes*. Let us denote the distance between consecutive nodes by dl . We shall refer to dl as the *leash length*. To avoid problems with self-penetration of the rope, dl must be smaller than $2R$.

The first and the last nodes are attached to walls, the distance between which is controlled. As SONO performs its job, the positions of the nodes become modified. This in general changes the distances between them. A *ControlLeashes* (CL) procedure built into the algorithm controls them. Let us explain how the control is performed.

CL checks the distance $d_{i,i+1}$ between the i and $i + 1$ nodes and corrects its length. Thus, if $d_{i,i+1} > dl$ then nodes i and $i + 1$ are symmetrically moved along the line which passes through

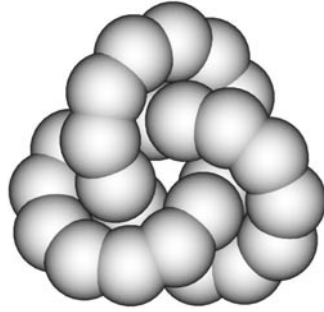


Figure 1. The rope used to simulate the knot is made of points which are surrounded by hard spheres of radius R .

them to positions at which $d_{i,i+1} = dl$. The action is realized by the following set of calculations:

$$\begin{aligned}
 d_{i,i+1} &= |\mathbf{r}_{i+1} - \mathbf{r}_i| \\
 \mathbf{e}_{i,i+1} &= \frac{\mathbf{r}_{i+1} - \mathbf{r}_i}{d_{i,i+1}} \\
 dd_{i,i+1} &= dl - d_{i,i+1} \\
 \mathbf{r}'_i &= \mathbf{r}_i - \frac{1}{2} dd_{i,i+1} \mathbf{e}_{i,i+1} \\
 \mathbf{r}'_{i+1} &= \mathbf{r}_{i+1} + \frac{1}{2} dd_{i,i+1} \mathbf{e}_{i,i+1}.
 \end{aligned}$$

The *CL* procedure starts at a randomly chosen node and runs, accordingly to the result of another random choice, up or down around the chain of nodes. Obviously, the *CL* procedure defined in such a manner is not self-consistent; after a single application the distances between consecutive nodes are not identical. However, its frequent application reduces the dispersion of the distances. The dispersion is constantly monitored by checking the value of the largest and smallest distances.

Nodes are points. To simulate a rope of radius R we assume that each of the points is surrounded by a hard sphere of radius R . See figure 1.

As the number N of the nodes is large and the distance dl between consecutive nodes is smaller than $2R$ the spheres surrounding consecutive nodes must be allowed to overlap. To achieve the aim, the hard core repulsion between the spheres is defined in a particular manner: spheres i and j repel each other only if their *index distance* $Id(i, j)$ is larger than a certain *skipped* integer. In an open knot, whose ends are separated spatially, the *index distance* between an i th and j th node is defined as $|j - i|$. A proper choice of the *skipped* parameter is crucial. It should be close to $round(\pi R/l)$. Removing overlaps which appear in the knot during its tightening process is the most time consuming task. It is performed by a *RemoveOverlaps* (*RO*) procedure. Before the procedure is called, one should find for each node all nodes which have a chance to overlap with it. This task is performed by a *FindNeighbours* (*FN*) procedure which updates an integer array $nn[1, \dots, N, 1, \dots, m]$, whose i th row contains indices of all nodes which are found within a distance smaller the $(2R + \varepsilon)$, where ε is a small parameter adjusted experimentally.

Assume that the nn array has been updated. Then, the *RO* procedure starts detecting and removing overlaps. The check starts at a randomly chosen node and, according to another

randomly chosen parameter, it runs up or down the chain of nodes. For a given i th node only the nodes whose indexes are found within the i th row of the nn array are checked for overlapping. If the spheres surrounding the i th and j th nodes are found to be overlapping, the nodes are shifted apart, symmetrically, along the line which joins their centres to a distance $(2R + \delta)$, where δ is another experimentally adjusted parameter. Putting $\delta > 0$ leaves some extra free space between the spheres shifted apart. As found experimentally, this speeds up the tightening process.

Removing an overlap between the i th and j th spheres can be performed by the following set of calculations:

$$\begin{aligned} d_{i,j} &= |\mathbf{r}_j - \mathbf{r}_i| \\ \mathbf{e}_{i,j} &= \frac{\mathbf{r}_j - \mathbf{r}_i}{d_{i,j}} \\ dd_{i,j} &= (2R + \delta) - d_{i,j} \\ \mathbf{r}'_i &= \mathbf{r}_i - \frac{1}{2} dd_{i,j} \mathbf{e}_{i,j} \\ \mathbf{r}'_j &= \mathbf{r}_j + \frac{1}{2} dd_{i,j} \mathbf{e}_{i,j}. \end{aligned}$$

The FN procedure is called much less frequently than the CL and RO procedures. Typically it is called only every 200 iteration steps. As in the case of the CL procedure, the RO procedure is not self-consistent. Removing overlaps between two nodes may create overlaps with other neighbours of the moved nodes; however, repeated use of the procedure asymptotically removes all overlaps (if the knot is not already tied too tight). The state of overlaps found within the chain is monitored by finding, during the run of the RO procedure, the values of the maximum and average overlaps.

2.2. Knot strength determination

The experiments aimed to determine the strength of different knots were carried out using a fishing line of nominal 100 N maximal tensile force. The fishing line has a diameter of 5×10^{-4} m, a linear density of 2.4×10^{-4} kg m $^{-1}$ and is made out of nylon. The Young's elastic modulus is in the range 2–4 GPa and the density is 1222 kg m $^{-3}$. Prior to the experiments, some grease was put on the fishing line in order to reduce the effects of friction. Then, at both ends of the fishing line, a figure-of-eight knot, made with the line doubled, was tightened, since the knots at the extremities must be stronger than the knots under test. The knots under test were always laced in the same manner to prevent the possibility that complex knots could assume different tight conformations. The fishing line was suitable to test the strength of the knots against each other, but to observe the rupture with a fast digital camera we had to use a much softer material. Spaghetti noodles were chosen because they come in the shape required and because, after cooking, they are soft, thus the rupture takes place slowly. The spaghetti was cooked in salty water (between 0.1 and 0.2 M NaCl) and the cooking time was long enough so that the spaghetti was well cooked. We have observed that well cooked spaghetti ruptures more reproducibly because surface defects are 'healed' out. To reduce the effect of friction, the spaghetti was lubricated with olive oil. The movies to observe the rupture of the knots on spaghetti were recorded using a colour digital camera Kodak HG-2000 with a recording speed of 1000 frames s $^{-1}$, and then transferred to a computer.

3. Results

The first experiments were dedicated to the determination of the relative ‘strength’ of the knots. To this end two different knots were tied side by side on the same cut of fishing line and the line was slowly stretched until breakage occurred. We observed that before breaking the knots adopted a very tight configuration and upon further increase of the tensile stress the line always broke within one of the knots, causing its subsequent unfolding, whereby the other knot remained intact. In order to ensure that the final form of the knot was always the same, care was taken to always tie the knots in the same way. Figure 2 shows the position of the ends during the tying of the different knots. This is important only for non-symmetric knots. In several trials of direct

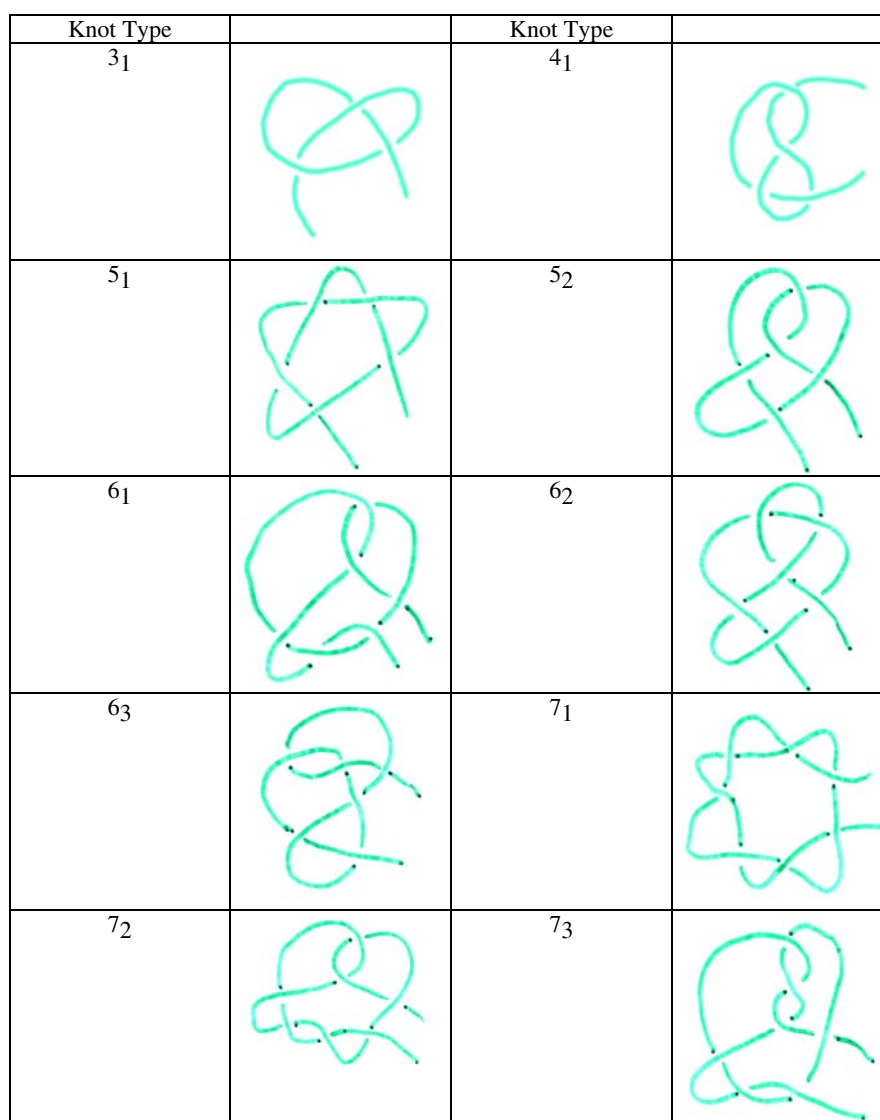



Figure 2. Using fishing line, each knot was tightened tied as depicted in this figure in order to prevent complex knots from forming different tight forms from one experiment to another.

Table 1. Knot strength as a function of the knot type. The knot strength increases from top to bottom of the table.

Knot type	Strength
3_1	
5_1	
5_2	
7_1	
6_1	
6_2	
6_3	
4_1	
7_2	
7_3	

competition between two different knots, the same one broke first as long as the knots were tied in the same way and adopted the same tight configuration. We compared the strength of knots 3_1 (overhand knot), 4_1 (figure-of-eight knot), 5_1 , 5_2 , 6_1 , 6_2 , 6_3 , 7_1 , 7_2 and 7_3 against each other (closed forms of these knots can be seen in standard tables of knots [8, 9] or in [10, 11]). Overhand knots turned out to be the weakest of all the knots.

In table 1 the different knot types are ordered by the increasing relative strengths resulting from direct competition. The results of table 1 show that generally the knot strength increases with knot complexity, with two exceptions: the figure-of-eight knot and 7_1 . If this rule is respected, it is clear that only the weakest knot can be determined by this direct competition procedure. Knot complexity can increase indefinitely and therefore we might never know the strongest ever possible knot. Since more complex knots can adopt different tight configurations, depending on the way they are tied, we decided to concentrate on the two most simple knots: overhand and figure-of-eight knots which, when tied on slippery fishing lines, always adopted the same form in their tight configuration. Of course the overhand knot always broke first in any direct competition with the figure-of-eight knot. Why do different knots break at different tensile stress? One of the primary changes imposed upon trajectories of knotted strings by their tight knotting is a high local curvature. In regions with high curvature strings are non-uniformly stressed. The side facing towards the outside of the bend is strongly stretched while the side facing towards the inside of the bend can even be compressed. When the string is, in addition, stretched by a tensile load, the side facing toward outside of the bend will reach the maximum rupture stress before any other part of the string. Crack formation at this point will lead to complete breaking of the string by transverse propagation of the fissure. Therefore, the higher the curvature, the lower the tensile load required for the crack formation. As even a very short region with a high curvature can initiate formation of cracks, one can expect that a string with a constant tensile load will break in the region with highest curvature. If that is indeed the case then the local curvature in tight overhand knots should reach a higher value than in tight figure-of-eight knots. As direct measurements of curvature in real, tight knots are dauntingly difficult, we resorted to simulations of tightly knotted trajectories of frictionless cylindrical tubes which are flexible (for bending) and radially non-compressible. To perform the simulation we used a modification of a previously described computer program of finding maximally tight trajectories

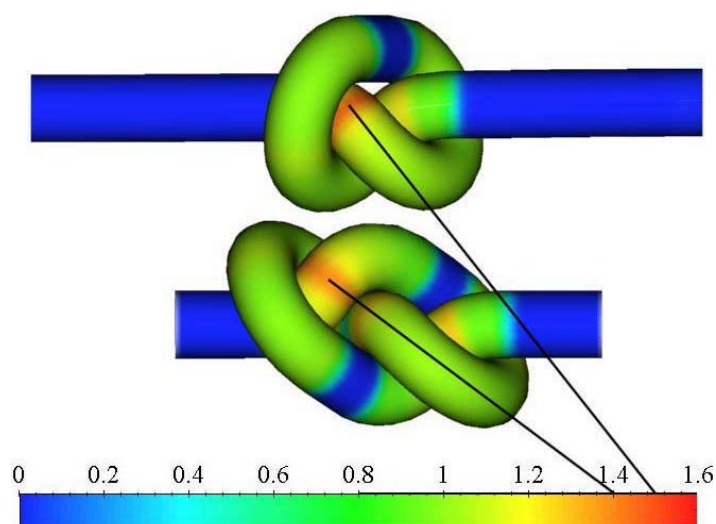


Figure 3. Tight trajectories of simulated overhand (upper) and figure-of-eight (lower) knots.

of closed knots [7, 12] as described in the methods section. Figure 3 shows tight trajectories of open overhand and figure-of-eight knot. The colour coding shows that regions with the highest curvature (red) are located on the inside of the knots, shortly after the string threads through the first external loop. The maximal curvature in a simulated tight overhand knot is indeed higher than in a tight figure-of-eight knot.

In figure 4 the curvature in the knots is plotted against the distance along the string. In this plot the maximal curvature for 3_1 is larger than the maximal curvature for 4_1 . It is also remarkable that the curvature peaks at a well defined position along the string. If curvature is the main cause of knot rupture, then one expects that the rupture is always at a well defined point along the string. Of course the simulated knots made of virtual strings having neither bending resistance nor friction and maintaining their circular cross section may differ from real knots tied on a fishing line, although fishing line shows a very low bending resistance and friction coefficient. To verify whether the regions with highest curvature correspond to sites where knotted fishing lines break and if indeed crack formation initiates in the outward facing side of the strongly bent regions, we decided to use a high velocity camera ($1000 \text{ images s}^{-1}$) to register sequential stages of knot breakage. However, fishing line breakage was so fast that from one image to another we observed a complete conversion from an intact tight knot to completely broken fishing line. Therefore, we decided to study breaking of knots tied on cooked spaghetti. Since cooked spaghetti has a much smaller Young's modulus, the process of breaking is relatively slow and we could register several hundred images from the apparition of an initial crack until the final breaking. However cooked spaghetti may behave differently from fishing lines. In particular, spaghetti can be easily broken by a strong bend while this is not the case of a fishing line. We investigated therefore the relative strength of overhand and figure-of-eight knots tied at the same time on spaghetti. At first, the results with spaghetti were not as clear cut as with fishing line. Overhand knots broke before figure-of-eight knots only in about 70% of cases. We interpret these results as a sign of non-homogeneity in spaghetti. When a weak spot (e.g. a pre-existing small defect) falls within one of the stretched regions of

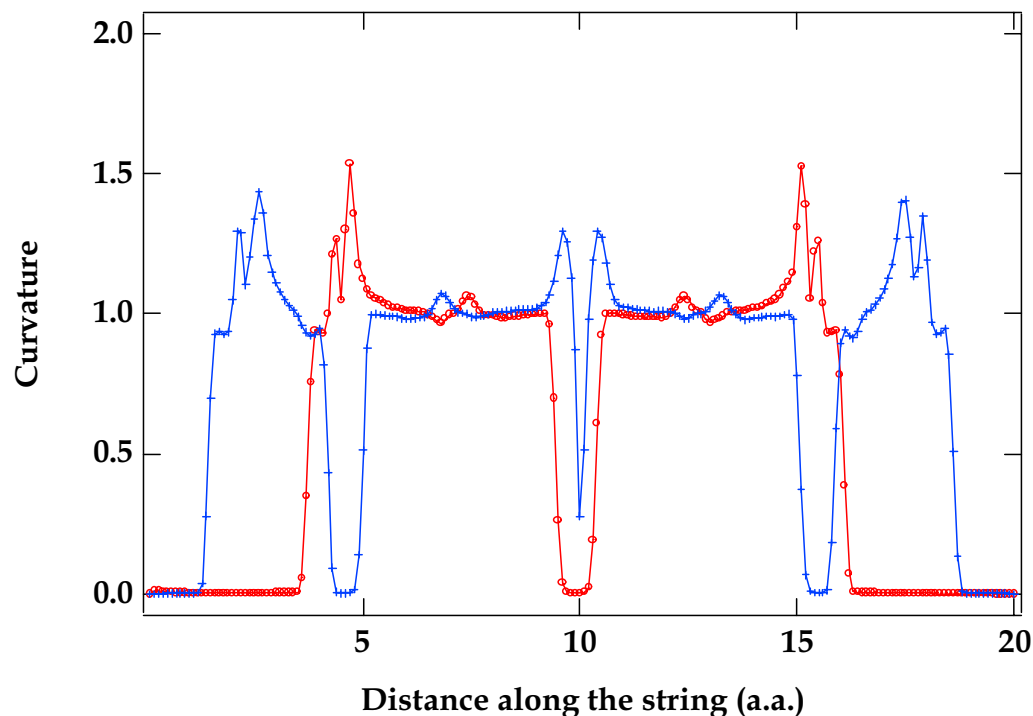


Figure 4. Curvature as a function of the position along the string: + denotes figure-of-eight and o denotes overhand knots. The curvature for the two knots has maxima, and in the case of the overhand knot the maximum value encountered along the knot is larger than that for the figure-of-eight knot. One also has to note that the maxima occur at well defined positions along the string.

figure-of-eight knots it may induce a breakage there under a force smaller than that required to break an overhand knot in its highly stretched regions but without weak spots. The problem was solved by cooking the spaghetti longer than for an ‘al dente’ preparation. Well cooked spaghetti has a surface which is softer and defects are ‘healed’ out in this way. After taking these precautions, we observed nearly 100% breakage of the overhand knot before the figure-of-eight knot. This fact indicates that the dynamics of the breakage process, fast in the case of the fishing line and slow for spaghetti, can only play a secondary role. Figure 5 shows a movie of the breakage in a spaghetti tied into an overhand knot. It is visible that tight overhand knots made of cooked spaghetti resemble the simulated tight overhand knot (figure 3) although a certain distortion, due to an elastic response of spaghetti, is apparent just before rupture. As expected, the crack originated in the outward facing side of the bend and propagated across the spaghetti. These results support our proposal that a high curvature correlates with the decreased strength of knotted strings. In these movies it is also clearly visible that the spaghetti is elastically deformed because the diameter of the spaghetti is reduced at the entrance to the knot. The same observations can be made for the rupture of a figure-of-eight knot, which is shown in figure 6. However, it is only a part of the story as the breakage did not occur in the internal region of the knot where the maximally tightened form shows its highest curvature (see figure 3). The breaking point for both knots was in the highly curved region, but localized closer to the entry to the knot.

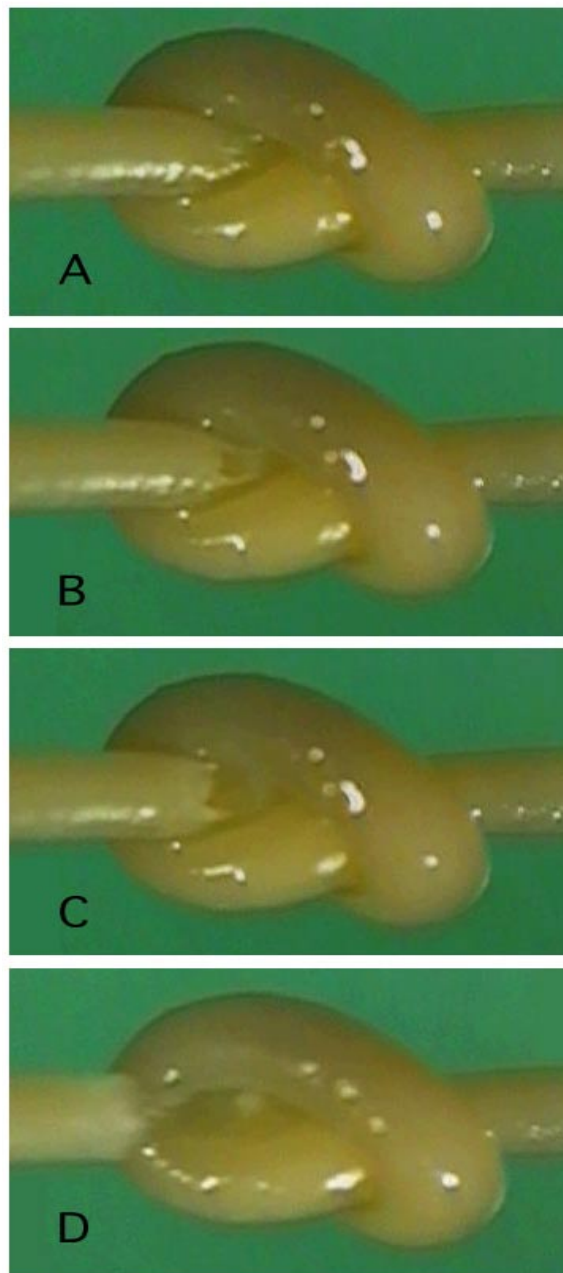


Figure 5. Movie of the rupture of an overhand knot tightened on spaghetti. The recording was made while gently pulling both ends of the knot by hand. The time lapse between the first sign of rupture of the knot and the complete separation of the two strings varied from 40 ms to 200 ms.

Up to now in our considerations we neglected the effect of friction on knot breakage. Tightening of real knots is opposed by increasing friction between segments that are pressed together. At some point this friction can be so strong that the string entering a knot will rather break than move further. Therefore real knots may never reach the maximally tight form which could be obtained with ideal frictionless tubes. Studies of the friction in knotted ropes [12]

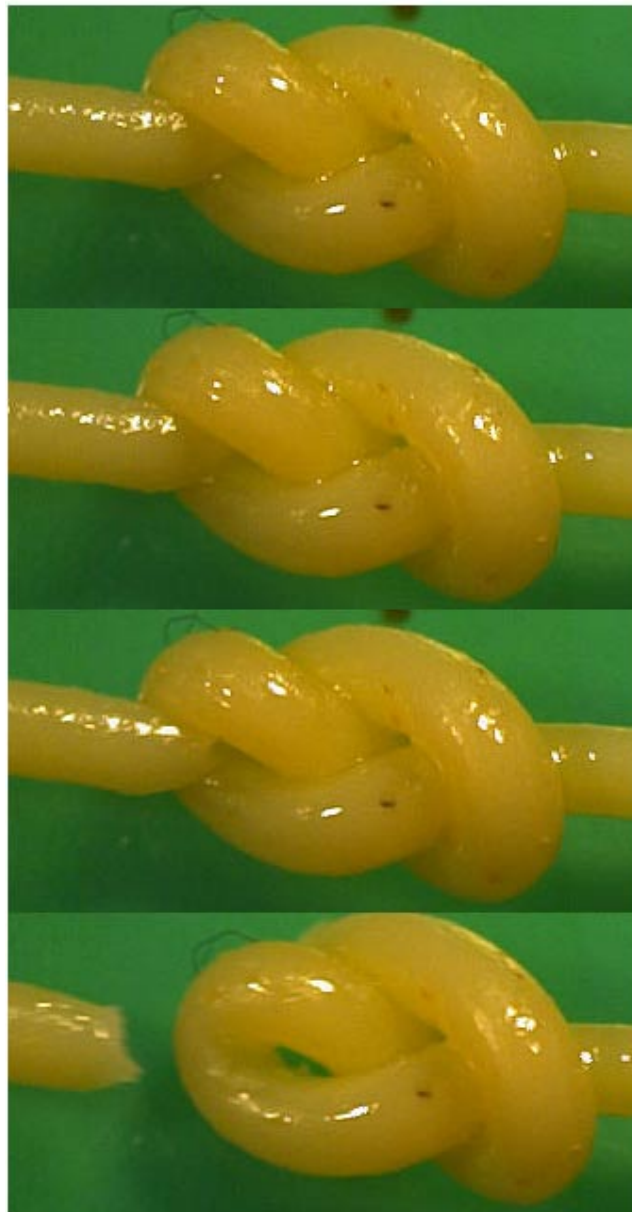


Figure 6. Movie of the rupture of a figure-of-eight knot tightened on spaghetti. The conditions of recording are similar to those of figure 5.

demonstrated that friction is greatly enhanced in the contact regions with high curvature. Therefore when the contribution of friction is not negligible the regions with high curvature at the entrance to the knot will effectively block further tightening of the knot. The level of possible tightening of real knots depends on factors such as the coefficient of inter-segmental friction and the strength of the material from which the knot is made. We decided to follow changes in the curvature of knots during their simulated tightening, although in our simulations friction was not present. Figure 7 shows sequential maps of curvature of a simulated overhand knot during its tightening and the simulated trajectories of overhand knots corresponding to the first and last curvature profiles obtained during progressive tightening. It is visible that both shapes can be

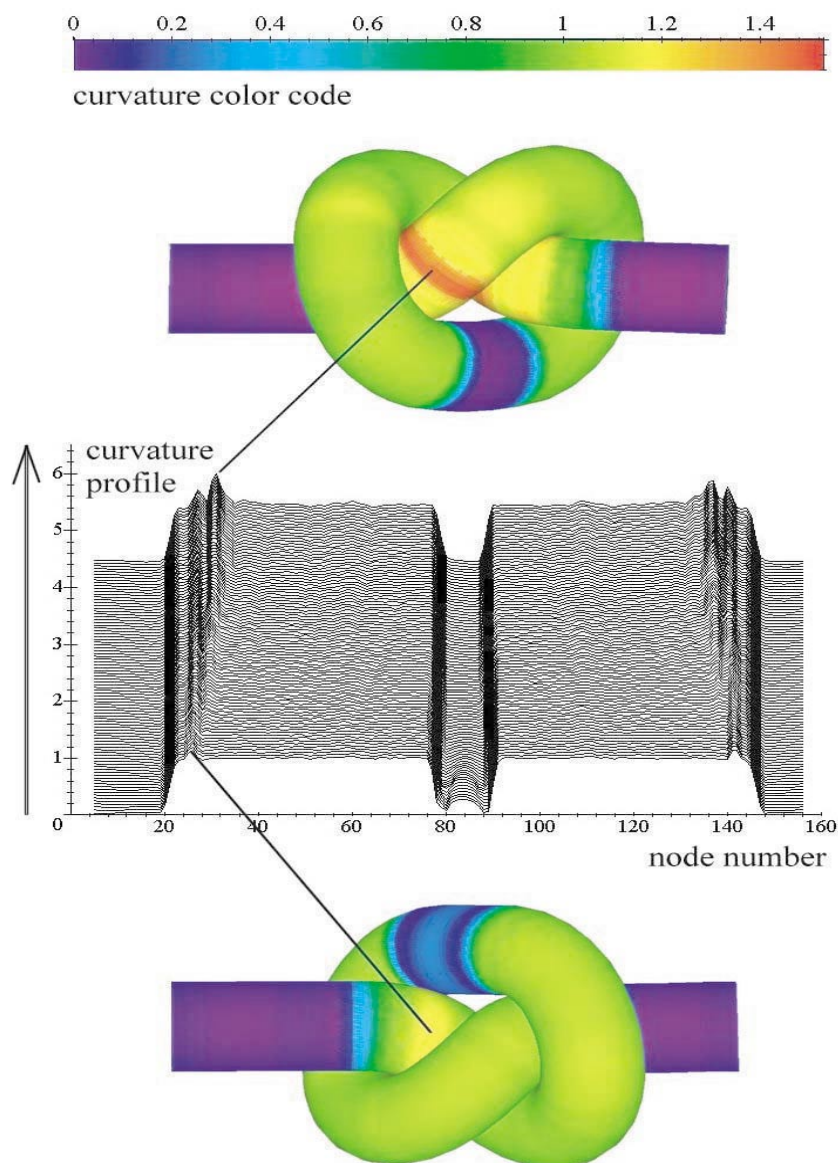


Figure 7. Curvature as a function of the position along the string and as a function of the tightening of the knot for an overhand knot. The curves are stacked by starting in front with the curve for a loose knot. One can observe that as tightening proceeds the maximum value of the curvature moves further into the knot.

considered as very tight and are practically indistinguishable upon visual inspection, however there are differences in the position of the regions with highest curvature (see the colour coding). In a slightly loosened knot the highest curvature is localized shortly after the entrance to the knot and its position corresponds to the experimentally observed breaking points in knotted spaghetti (see figures 5 and 6). In the maximally tight state (that may be only accessible to very slippery materials such as fishing lines) the region of highest curvature is localized deeper in the knot.

Friction has also another important effect on the tension within a knot. Figure 8 schematically illustrates how the friction affects the redistribution of tensile load and thus of

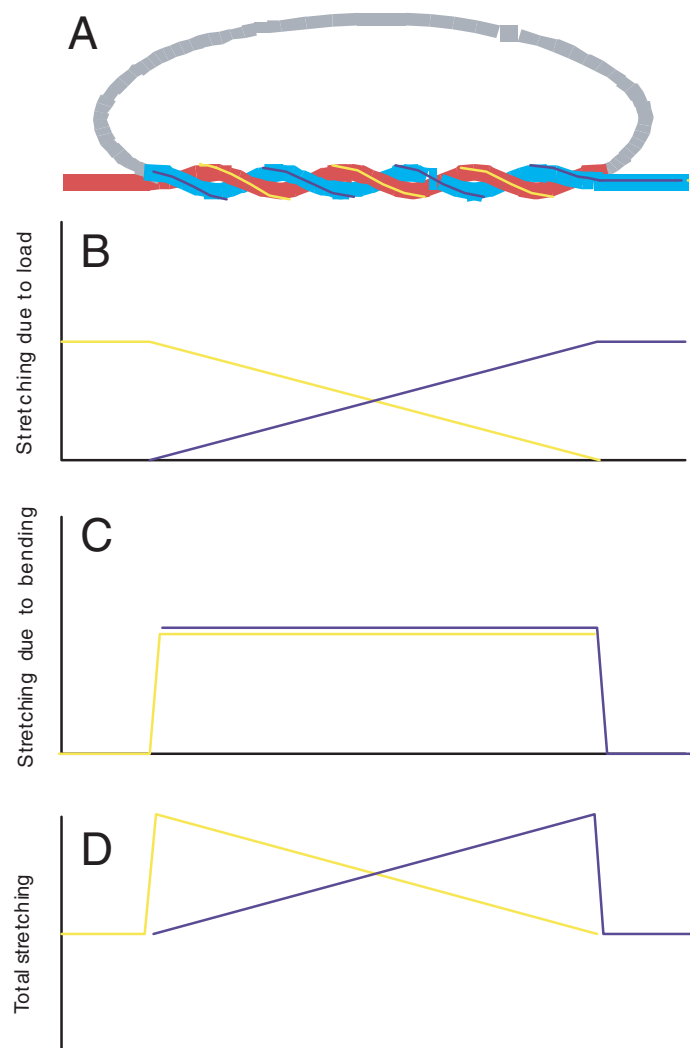


Figure 8. A, stretching of the string along the knot shown in A. B, stretching due to the load applied at the ends of the knot. C, stretching due to bending. D, sum of the stretching due to load and to bending.

load-induced stretching in the tightly intertwined region at the base of a knotted loop. It is apparent that before entering into the intertwined region each rope is under the total load. Upon entering the intertwined region the load becomes progressively redistributed between the two ropes due to the effect of friction. Thus in the central portion of the intertwined region each rope is only under half of the total tensile load. Since stretching caused by the load adds to that caused by the bending, and, in the case of a constant bending of the intertwined region (as that in figure 8), the rope under an increasing load will eventually break at one of the entries in to the intertwined region. In addition, the break should start on the side being stretched by bending. Therefore even if the curvature-induced stress inside the knot would exceed the stress at the entrance, the knotted string is more likely to break close to the entrance since it is under a higher tensile load.

A recent study addressed, by molecular simulations, the influence of knotting on the strength of an individual polyethylene chain [4]. It is striking that the polyethylene chain breakage point (figures 1 and 4 in [3]) localizes in the overhand knot at the same place where we observe the breakage of the knotted spaghetti (see figure 5). This agreement between simulations performed at the atomic level and macroscopic experiments with knotted spaghetti is spectacular.

Acknowledgments

We thank Beat Kneubuehl and Fritz Trösch of the Swiss Defense Procurement Agency for making available the high-speed camera. We thank Hiroki Uehara for sharing unpublished data on knot breakage. We also thank Gregory Buck and François Rothen for valuable discussions. This work was supported by the Swiss National Foundation for grants to JD and AS (grant number 31-61636.00), S Catsicas and SK and to GD (grant number 21-54003.98), and the Polish Committee of Scientific Research (grant number KBN 8T11F01214) and the Herbette Foundation with a grant to PP.

References

- [1] Ashley C W 1993 *The Ashley Book of Knots* (New York: Doubleday)
- [2] Stasiak A, Dobay A, Dubochet J and Dietler G 1999 *Science* **286** 11a
- [3] Arai Y, Yasuda R, Akashi K-i, Harada Y, Miyata H, Kinoshita K Jr and Itoh H 1999 *Nature* **399** 446
- [4] Saitta A M, Soper P D, Wasserman E and Klein M L 1999 *Nature* **399** 46
- [5] Taylor W R 2000 *Nature* **406** 916
- [6] Yan J, Magnasco M O and Marko J F 1999 *Nature* **401** 932
- [7] Pieranski P 1998 *Ideal Knots* ed A Stasiak, V Katritch and L H Kauffman (Singapore: World Scientific) p 20
- [8] Rolfsen D 1976 *Knots and Links* (Berkeley, CA: Publish or Perish)
- [9] Adams C 1994 *The Knot Book* (New York: Freeman)
- [10] Katritch V, Bednar J, Michoud D, Sharein R G, Dubochet J and Stasiak A 1996 *Nature* **384** 142
- [11] Katritch V, Olson W K, Pieranski P, Dubochet J and Stasiak A 1997 *Nature* **388** 148
- [12] Maddocks J H and Keller J B 1987 *SIAM J. Appl. Math.* **47** 1185